Versão do arquivo anexado / Version of attached file:

Versão do Editor / Published Version

Mais informações no site da editora / Further information on publisher's website:

https://www.sciencedirect.com/science/article/pii/S2468519423002343

DOI: https://doi.org/10.1016/j.mtchem.2023.101607

Direitos autorais / Publisher's copyright statement:
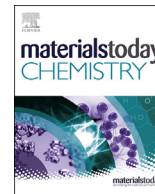
Electrolyte precursor–free approach to prepare composite electrolyte for all-solid-state Na-ion battery

L. He [a], Z. Wang [b], Y. Li [c, ***], H. Lin [d], J. Li [e], T. Cheng [a], Q. Zhu [b], C. Shang [b], Z. Lu [b, **], R. Floriano [f], H.-W. Li [a, *]

[a] *Hefei General Machinery Research Institute Co., Ltd, Hefei 230031, China*
[b] *Department of Materials Science and Engineering, Southern University of Science and Technology, Shen Zhen 518055, China*
[c] *School of Materials Science and Engineering, Anhui University of Technology, Maanshan 243002, China*
[d] *Institute of Advanced Wear & Corrosion Resistance and Functional Materials, Jinan University, Guangzhou 510632, China*
[e] *Huzhou Key Laboratory of Materials for Energy Conversion and Storage, School of Science, Huzhou University, Huzhou 313000, China*
[f] *School of Applied Sciences, University of Campinas (FCA-UNICAMP), Pedro Zaccaria, 1300, Limeira 13484-350, Brazil*

ARTICLE INFO

ABSTRACT

Composite electrolytes with higher conductivities have been widely studied, aiming at application to advanced all-solid-state batteries with good safety and high energy density. Most composite electrolytes are prepared via physical blend of electrolyte precursors or modification/doping/reaction based on one of them, which may confine people's scope for the further development of advanced solid electrolytes. Herein, we first prepare composite electrolytes via sophisticated design of chemical reaction without using any electrolyte precursors. Chemical reaction between NaNH$_2$ and B$_{10}$H$_{14}$ is successfully used to synthesize NaBH$_4$-Na$_2$B$_{12}$H$_{12}$ composite electrolyte with special core-shell structure. Importantly, the NaBH$_4$-Na$_2$B$_{12}$H$_{12}$ composite electrolyte synthesized via electrolyte precursor–free approach exhibits a high ionic conductivity of 1×10^{-4} S/cm at 373 K-over 1 (or 4) magnitude higher than the bulk Na$_2$B$_{12}$H$_{12}$ (or NaBH$_4$) and excellent electrochemical stability up to 5 V (vs. Na$^+$/Na). All-solid-state Na-ion battery using the as-synthesized composite electrolyte can reversibly work more than 100 cycles with capacity retention of 75.4 mAh/g at 348 K and 0.1°C. This work sheds new lights on the preparation of more advanced composite electrolytes.

© 2023 Published by Elsevier Ltd.

1. Introduction

With the broader application of lithium-ion batteries, their low operational safety deriving from using flammable organic liquid electrolytes has been arousing more and more vigilance from all over the world. Rechargeable all-solid-state battery with high safety and energy density is suggested as an effective solution to the issues of traditional batteries using liquid electrolytes. The remarkable difference between all-solid-state batteries and traditional batteries is the former adopts solid electrolytes, whereas the latter adopts liquid ones; therefore, the properties of solid electrolytes play an important role in the performance of as-assembled all-solid-state batteries.

Usually, solid electrolytes have room temperature conductivities far less than that of liquid electrolytes at the magnitude of 0.01 S/cm, which hampers the practical application for all-solid-state batteries [1–4]. In recent years, sulfides and oxides electrolytes with high ionic conductivities comparable to those of liquid electrolytes have been successively reported; nevertheless, their stabilities or poor interfacial contact are encountering challenges [5–10]. A new type of stable solid electrolyte-complex hydrides, owning favorable mechanical properties and high conductivities above their phase transition temperatures, are one of the most promising solid electrolyte materials if their high-temperature phases can be stabilized at relatively low temperature [4,11–13].

To obtain electrolyte materials with both outstanding conductivity and stability for all-solid-state battery application, preparation of composite electrolytes is becoming a very important and popular approach. Many kinds of composite electrolytes have been

---

prepared, and they can be easily divided into two categories: inorganic-organic composite electrolytes such as PEO-NaPF$_6$ [14], TiO$_2$-PEO-NaClO$_4$ [15], NASICON-PVdF-HFP-ether [16]; and inorganic-inorganic composite electrolytes such as LiBH$_4$-P$_2$S$_5$ [13], LiBH$_4$-LiCl [17], LiBH$_4$-SiO$_2$ [18], Na$_3$PS$_4$-Na$_4$SiS$_4$ [19], Li$_3$PS$_4$-LiI [20], Na$_3$NH$_2$B$_{12}$H$_{12}$, Li/NaCB$_9$H$_{10}$-Li/NaCB$_{11}$B$_{12}$ [22], conjuncto-hydroborate [23—29], Li$_7$La$_3$Zr$_2$O$_{12}$ [2], NASICON [30—33], and others [34—37]. Traditional preparation method of these composite electrolytes can be simply depicted using equation (1):

$$A + B \rightarrow AB \qquad (1)$$

In mode (1), composite electrolytes are usually obtained by physical blend of electrolyte precursors A and B (e.g. LiBH$_4$-LiCl and Na$_2$B$_{10}$H$_{10}$-Na$_2$B$_{12}$H$_{12}$) or decoration of precursor A using B as additive/dopant/modifier (e.g. PEO-NaPF$_6$ and LiBH$_4$—SiO$_2$) followed by sintering at appropriate temperatures. Many of them exhibit optimized performance, and more and more similar research using the same strategy are reported, which may result in confining the further development of composite electrolytes. The notable character of mode (1) is that no valence change happens during composite electrolytes (AB) preparation processes and the electrolyte precursor units still exist in AB.

Composite electrolytes are so widely used in batteries; one may ask, "Whether there is another alternative strategy for composite electrolytes preparation?" It triggers us to investigate the possibility to prepare composite electrolytes via a completely novel approach, that is, synthesis via sophisticated design of chemical reaction. To distinguish it from mode (1), it is simply depicted using equation (2) as follows:

$$C + D \rightarrow AB \qquad (2)$$

In mode (2), valence states of partial elements change during the formation process of AB from non-precursor compounds C and D. The comparison of mode (1) and (2) is shown in Fig. 1; the colors represent different materials, and the shapes describe their distribution state. By the comprehensive consideration of cost (Na is much cheaper than Li), stability, ionic conductivity, and large-scale energy storage, as a case study, Na$_2$B$_{12}$H$_{12}$ was finally chosen as B for its outstanding performance in composite electrolytes [4,23—25,38]. To design reaction (2), it is expected that A has certain similarity to B for both A and B are transformed from C and D; and A is preferable to be the precursor of B and can in situ react with C or D to produce B. If either condition is fulfilled, reaction (2) can be well designed. Inspired by the solid reaction between M(BH$_4$)$_n$ (n is the valence of metal M) and B$_{10}$H$_{14}$ for M$_{2/n}$B$_{12}$H$_{12}$ synthesis [39—42] and the high conductivity of Na$_3$BH$_4$B$_{12}$H$_{12}$ [23,38] and Na$_3$NH$_2$B$_{12}$H$_{12}$ [21] composite electrolytes, A is set as NaBH$_4$ and D as B$_{10}$H$_{14}$. C should be the material, which can react with B$_{10}$H$_{14}$ to produce NaBH$_4$; based on the reported literature [43], NaNH$_2$ with relatively fine safety and low cost was eventually adopted for the case study. Because both NaBH$_4$ and Na$_2$B$_{12}$H$_{12}$ are the reaction products of NaNH$_2$ and B$_{10}$H$_{14}$, moreover, NaBH$_4$ will further form Na$_2$B$_{12}$H$_{12}$ under the reaction with B$_{10}$H$_{14}$, and the composite electrolytes NaBH$_4$-Na$_2$B$_{12}$H$_{12}$ with higher ionic conductivity are hopeful to be synthesized via simple adjustment of the stoichiometric ratio of NaNH$_2$:B$_{10}$H$_{14}$.

2. Experimental

Commercial B$_{10}$H$_{14}$ (98%; 3B Scientific) and NaNH$_2$ (99%; ThermoFisher Scientific) were purchased and stored in Ar glove box for direct experimental use. Reactants NaNH$_2$ and B$_{10}$H$_{14}$ were weighed according to different stoichiometric ratios and then milled using pestle and agate mortar for 30 min at room temperature under 1 atm Ar pressure to form uniform mixtures. Subsequently, the uniform mixtures were put into (~2.8 cm^3) stainless steel crucibles for heat treatment with different reaction temperatures and times. The products after heat treatment were collected for analysis, and all the sample preparation was conducted in Ar glove box.
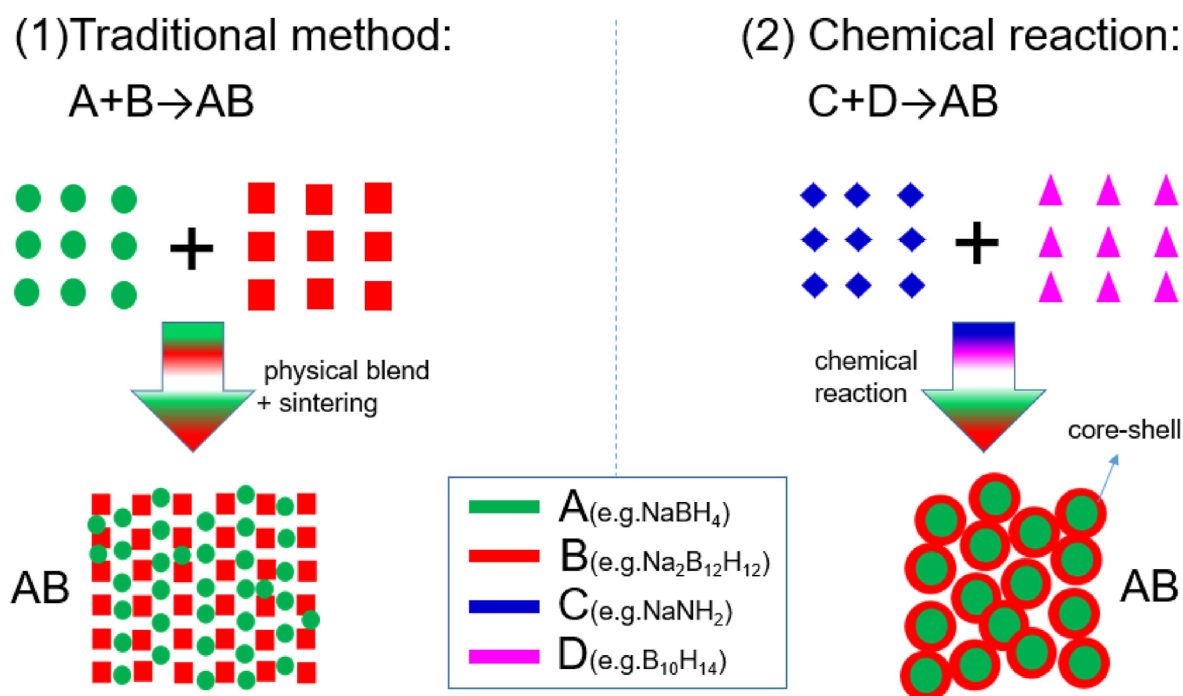

Fig. 1. Schematic illustration of composite electrolytes AB prepared via traditional method and electrolyte precursor—free chemical reaction (A = precursor 1; B = precursor 2 or additive/dopant/modifier; C = non-precursor compound 1; D = non-precursor compound 2).

Rigaku SmartLab X-ray diffractometer with Cu-Kα radiation ($\lambda = 1.5418$ Å) was used to collect the X-ray diffraction patterns, and accelerating voltage/tube current was set as 45 kV/200 mA.

The samples were smoothly placed in quartz glass plate followed by sealing using Scotch tape in Ar glove box to prohibit air contamination during measurement process. Raman spectra were collected using a 532 nm of laser wavelength on Horiba Raman Spectrometer. To well exhibit all the B-H vibrations, the wavenumber range was set as 100−4,000 cm.

Solid-state ^{11}B MAS NMR spectra were obtained from a Bruker Advance 500 MHz spectrometer using a MAS probe of 4 mm with a magnet of 11.7 T. The ^{11}B nuclei spectral frequency was set as 160.50. An 8 kHz of single pulse (0.5 μs-π/12) ^{11}B MAS NMR experiment was performed with strong ^{1}H decoupling. NMR shifts are referenced to BF$_3$•Et$_2$O ($\delta = 0.00$ ppm) as standard sample for ^{11}B NMR. The samples were put into a ZrO$_2$ rotor (4 mm diameter) and sealed with airtight Kel-F cap in Ar glove box. Dry N$_2$ was used for sample spinning. PeakFit 4.12 software with a Gaussian response function was used to perform the peak deconvolution of ^{11}B MAS NMR curves, and the related coefficient (r^2) is higher than 0.99.
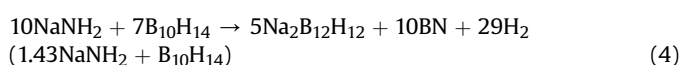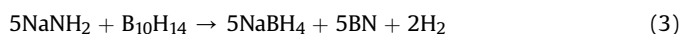
The ionic conductivity was collected using electrochemical impedance spectroscopy. The sample was tablet compressed into a 1 mm/8 mm (thickness/diameter) pellet at 20 MPa for 12 h. Nine-micrometer thickness of Cu foils were adopted as electrodes, and they were mechanically pasted on two sides of the pellet in 2025 coin cell. Zahner-Elektrik IM6ex electrochemistry workstation was used to collect impedance plots, and the frequency range was set as 1 Hz to 1×10^6 Hz.

Cyclic voltammetry (CV) was completed on Zahner-Elektrik IM6ex electrochemistry workstation, and the scanning rate and voltage range were set as 10 mV/s and −1 V to 5 V. The electrolyte powder was vertically pressed into 35 MPa for 12 h in an 8 mm die (diameter). The as-prepared pellet was used as solid electrolyte, and Pt and Na were used as positive and negative electrodes, respectively. They were sealed into an airtight coin cell for CV analysis.

The property of all-solid-state battery was measured with Neware battery test system via galvanostatic charge/discharge measurements at 348 K and 1.0 to ~2.5 V (vs. Na$^+$/Na). TiS$_2$ is mixed with 1.43:1-HT in a 60:40 wt% ratio by hand milling for 0.5 h to prepare TiS$_2$/1.43:1-HT powder. Then the TiS$_2$/1.43:1-HT powder was adopted as mixture cathode and pressed together with 1.43:1-HT solid electrolyte powder at 35 MPa for 12 h to fabricate a composite pellet with electrolyte and positive electrode. Na foil was then pasted to the produced pellet as negative electrode, and they were sealed into a 2025 coin cell to make TiS$_2$/1.43:1-HT | 1.43:1-HT | Na battery for battery property analysis.

3. Results and discussion

Electrolyte synthesis is based on the chemical reaction as illustrated in Fig. 1(2) and follows the reaction paths (3) and (4) as previously reported [43].

$$5NaNH_2 + B_{10}H_{14} \rightarrow 5NaBH_4 + 5BN + 2H_2 \qquad (3)$$

$$10NaNH_2 + 7B_{10}H_{14} \rightarrow 5Na_2B_{12}H_{12} + 10BN + 29H_2$$
$$(1.43NaNH_2 + B_{10}H_{14}) \qquad (4)$$

Nevertheless, neither Equation (3) nor Equation (4) independently occurs because the produced NaBH$_4$ simultaneously reacts with B$_{10}$H$_{14}$ to form Na$_2$B$_{12}$H$_{12}$ as described in Equation (5) [39]:

$$2NaBH_4 + B_{10}H_{14} \rightarrow Na_2B_{12}H_{12} + 5H_2 \qquad (5)$$
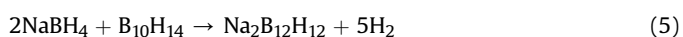
This special reaction property between NaNH$_2$ and B$_{10}$H$_{14}$ is harmful for synthesizing NaBH$_4$ or Na$_2$B$_{12}$H$_{12}$ with highest purity but facilitates to prepare a series of NaBH$_4$-Na$_2$B$_{12}$H$_{12}$ co-existing composite electrolytes. The mol ratio of NaBH$_4$:Na$_2$B$_{12}$H$_{12}$ can be easily manipulated by adjustment of relative mol amount of starting materials of NaNH$_2$ and B$_{10}$H$_{14}$. With peak fitting of ^{11}B MAS NMR spectra (Fig. S1), the mol ratio change of NaBH$_4$ to Na$_2$B$_{12}$H$_{12}$ as a function of relative mol ratio (x:1) of NaNH$_2$:B$_{10}$H$_{14}$ is shown in Fig. 2.

It is shown that the sintered 5NaNH$_2$+B$_{10}$H$_{14}$ sample (x = 5, marked as 5:1-HT, similarly hereinafter) results in 38.36:1 of NaBH$_4$ to Na$_2$B$_{12}$H$_{12}$ [43], and with the increase of B$_{10}$H$_{14}$ content, the mol ratio of NaBH$_4$ to Na$_2$B$_{12}$H$_{12}$ monotonously decreases, which indicates the second step reaction of B$_{10}$H$_{14}$ for Na$_2$B$_{12}$H$_{12}$ production via Equation (5). In 2:1-HT and 1.43:1-HT samples, the mol ratios of NaBH$_4$ to Na$_2$B$_{12}$H$_{12}$ are 5.22:1 and 1.96:1, respectively (Table S1). In 1:1-HT sample, the content of Na$_2$B$_{12}$H$_{12}$ reaches highest, and the mol ratio of NaBH$_4$ to Na$_2$B$_{12}$H$_{12}$ is as low as 1.09:1 [43]. The interesting change tendency of relative content of NaBH$_4$ to Na$_2$B$_{12}$H$_{12}$ triggers us to investigate the conductive behaviors of a series of NaBH$_4$-Na$_2$B$_{12}$H$_{12}$ composite electrolytes synthesized by chemical reaction of xNaNH$_2$+B$_{10}$H$_{14}$.

The temperature dependencies of ionic conductivity (σ) of a series of samples prepared by sintering xNaNH$_2$+B$_{10}$H$_{14}$ are shown in Fig. 3. Alternating current (AC) impedance measurements in a frequency range of 1 Hz to 1 MHz and temperature range of 273 K−373 K were adopted (Fig. S2). The conductivities of synthesized samples varied greatly with the change of x. When x is 0.5, the σ is about two orders of magnitude lower than that of Na$_2$B$_{12}$H$_{12}$, which is attributed to the harmful influence of excess B$_{10}$H$_{14}$ on the conductivity of produced Na$_2$B$_{12}$H$_{12}$ [43]. While x becomes 5, the main products are NaBH$_4$ and BN (Fig. S3a and b), and the σ is more than one order of magnitude higher than that of bulk NaBH$_4$ [44], which means the introduction of BN may facilitate to improve the conductivity of NaBH$_4$. Both 1:1-HT and 2:1-HT samples exhibit conductivities several times higher than that of Na$_2$B$_{12}$H$_{12}$. Particularly, 1.43:1-HT sample is found to present the highest conductivity, and it is around one order of magnitude higher than that of Na$_2$B$_{12}$H$_{12}$ and reaches 1.2×10^{-6} and 1×10^{-4} S/cm at 298 and 373 K, respectively.

To understand the behaviors of Na$^+$ ion conductivity, 5:1-HT and 1.43:1-HT samples as representatives were collected for X-ray diffraction analysis (XRD), Raman, and transmission electron microscopy (TEM) measurements, as shown in Figs. S3 and S4. In Fig. S3, XRD indicates the main formation of NaBH$_4$, and Raman indicates strong vibration peaks of BN and NaBH$_4$, which means the amorphous morphology of produced BN [45]. TEM images of 5:1-HT indicate spherical particles of formed NaBH$_4$-BN composite
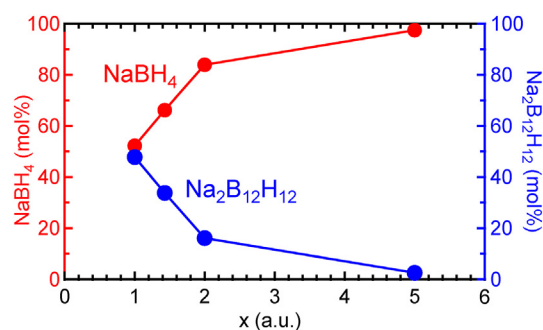
Fig. 2. The change tendency of relative proportion (mol%) of NaBH$_4$ and Na$_2$B$_{12}$H$_{12}$ as a function of x (x represents the mol ratio value of starting materials NaNH$_2$:B$_{10}$H$_{14}$, 573 K for 10 h) [43].
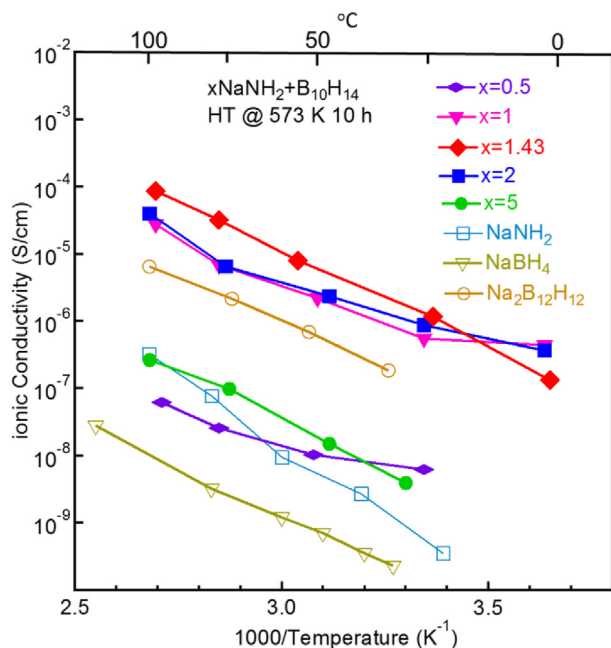
Fig. 3. Ionic conductivity measurements for a series of samples synthesized via heat treatment of $xNaNH_2+B_{10}H_{14}$ at 573 K for 10 h $NaBH_4$ [44], $Na_2B_{12}H_{12}$ [40], and starting material $NaNH_2$ are also shown for references.

with ca. 200−350 nm size (Fig. S3c). With greater magnification, lattice fringe with 0.35 nm of width from $NaBH_4$ (111) (Fig. S3f) with different growth directions (Fig. S3d and e) and amorphous BN can be clearly observed, which support the XRD and Raman results and reveal the elevated conductivity is derived from the formation of glass phase of $NaBH_4$ dispersed in amorphous BN, as the formation of glass phases was reported to facilitate ionic conductivity [5,46]. In Fig. 4, XRD shows apparent diffraction signals of $NaBH_4$ and $Na_2B_{12}H_{12}$, whereas Raman only shows the vibration peaks of $Na_2B_{12}H_{12}$, which implies $Na_2B_{12}H_{12}$ may distribute on the surface of $NaBH_4$ and the signal of $NaBH_4$ inside is shielded by $Na_2B_{12}H_{12}$ [43]. TEM images of 1.43:1-HT indicate spherical particles with special core-shell structure with a core diameter of 117 nm and shell diameter of 160 nm (Fig. 4c). The result is in accordance with the XRD and Raman analysis and confirmed the speculation that the external part of sphere is $Na_2B_{12}H_{12}$ and the internal part is $NaBH_4$. With greater magnification, the core shows amorphous morphology with ambiguous lattice fringes similar to sample 5:1-HT, whereas the shell shows obviously larger lattice fringes with 0.436 nm width originated from $Na_2B_{12}H_{12}$ (111). The observation further confirms the two-step reaction of Equation (4) via Equations (3) and (5). The excess $B_{10}H_{14}$ further reacts with as-formed $NaBH_4$ sphere on its surface and results in special core-shell structure of $NaBH_4$-$Na_2B_{12}H_{12}$ composite electrolyte (Fig. 1); it is much different from general composite electrolytes usually prepared via physical blend followed by sintering. The similar core-shell structure of $NaBH_4@Na_2B_{12}H_{12}$ with ionic conductivity of
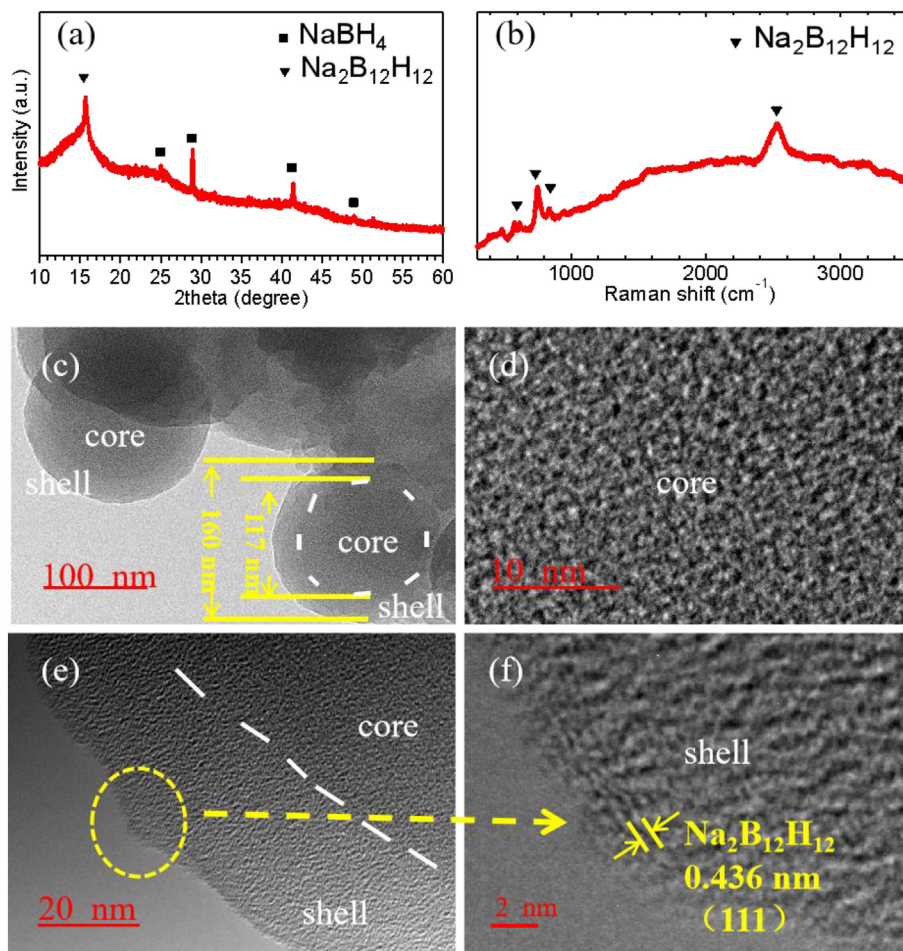

Fig. 4. XRD pattern (a), Raman spectrum (b) [43], and TEM images (c, d, e, and f) of 1.43:1-HT sample.

Table 1
Comparison of the Na$^+$ conductivities of NaBH$_4$-Na$_2$B$_{12}$H$_{12}$ composite electrolytes prepared by different methods.

Name of NaBH$_4$-Na$_2$B$_{12}$H$_{12}$ composite electrolyte	Conductivity at 298 K (S/cm)	Conductivity at higher temperatures (S/cm)	Preparation methods	References
Na$_3$BH$_4$B$_{12}$H$_{12}$	5×10^{-4}	4×10^{-3} @369 K	Physical blend + heat treatment	[23]
NaBH$_4$@Na$_2$B$_{12}$H$_{12}$	4×10^{-6}	1×10^{-4} @388 K	Partial chemical modification	[38]
1.43:1-HT	1.2×10^{-6}	1×10^{-4} @373 K	Full chemical reaction	This work

1×10^{-4} S/cm at 388 K was recently reported by Luo et al., and they used excess NaBH$_4$ as precursor and toxic gas B$_2$H$_6$ as reactant (mode 1) to partially modify NaBH$_4$ on its surface [38]. In fact, NaBH$_4$-Na$_2$B$_{12}$H$_{12}$ composite electrolyte was first prepared by Sadikin et al. by ball milling of 1:1 mol of NaBH$_4$ and Na$_2$B$_{12}$H$_{12}$, and the as-prepared Na$_3$BH$_4$B$_{12}$H$_{12}$ is stable to 298 K with 5×10^{-4} S/cm Na$^+$ conductivity [23]. The difference is that electrolyte precursors are not needed in the present study because both NaBH$_4$ and Na$_2$B$_{12}$H$_{12}$ are in situ produced by chemical reaction (mode 2), and we propose a completely different and novel strategy to design and prepare composite electrolyte here. The Na$^+$ conductivities of NaBH$_4$-Na$_2$B$_{12}$H$_{12}$ composite electrolytes prepared by different methods are compared in Table 1. The conductivities of NaBH$_4$-Na$_2$B$_{12}$H$_{12}$ prepared by chemical methods seem to be lower than that by physical method at present, and it may originate from the incomplete reaction and by-products during chemical processes [43]. The conductivity is hopeful to be further improved by optimization of reaction conditions in the future.

Excess B$_{10}$H$_{14}$ reacts with as-formed NaBH$_4$ on the surface of produced NaBH$_4$ particles, which results in in situ production of NaBH$_4$-Na$_2$B$_{12}$H$_{12}$ composite electrolyte with intimate contact in core-shell structure. The intimate contact increases the conductivity of NaBH$_4$-Na$_2$B$_{12}$H$_{12}$, similar to the reported Na$_2$(B$_{10}$H$_{10}$)(B$_{12}$H$_{12}$) composite electrolyte [24,25]. The results show in situ synthesis of composite electrolytes is an effective new strategy for the preparation of electrolytes with higher conductivity, better molecule contact, and special morphology. Advanced composite electrolytes with super-fine stability and conductivity are probably synthesized by this method via reasonable design, e.g. using LiH (or NaH) to react with B$_{10}$H$_{14}$ may produce Li$_2$B$_{12}$H$_{12}$ (or Na$_2$B$_{12}$H$_{12}$)-included [39] composite electrolytes avoiding the interruption of BN in the future.

^{11}B MAS NMR spectra (Fig. S4) show the practical composition of 1.43:1-HT sample, and it is found that the main component is Na$_2$B$_{12}$H$_{12}$ (74.3 wt%/1 mol) and the others are NaBH$_4$ (7.3 wt%/0.488 mol), Na$_2$B$_{10}$H$_{10}$ (9.8 wt%/0.151 mol), and BN (8.5 wt%/0.866 mol). [B$_{10}$H$_{10}$]$^{2-}$ as a side product in the process of preparation of [B$_{12}$H$_{12}$]$^{2-}$ has been many reported [39,41,47]. In recent years, M$_2$B$_{10}$H$_{10}$ (M = Li, Na) has been proved to show better ionic conductivity than that of M$_2$B$_{12}$H$_{12}$, and stable composite electrolyte Na$_2$(B$_{12}$H$_{12}$)$_{0.5}$(B$_{10}$H$_{10}$)$_{0.5}$ has been successfully applied for a stable all-solid-state Na-ion battery [25]. In this study, the high conductivity of 1.43:1-HT sample may derive not only from the formation Na$_2$B$_{12}$H$_{12}$-NaBH$_4$ core-shell structure but also the partial formation of small amount of Na$_2$B$_{12}$H$_{12}$-Na$_2$B$_{10}$H$_{10}$, as both composite electrolytes have elevated ionic conductivities [23,26]. The activation energy Ea for Na ionic conduction of 1.43:1-HT sample was calculated from the slopes of Arrhenius plots as 0.59 eV, which is in good agreement with Na$_2$B$_{12}$H$_{12}$-Na$_2$B$_{10}$H$_{10}$ (0.56−0.64 eV) composition [26], which supports the aforementioned speculation well. In future work, reaction conditions will be optimized to be apt to produce Na$_2$B$_{10}$H$_{10}$, and the conductivity of as-produced composite electrolytes is hopeful to be further improved.

With the highest conductivity among all the synthesized samples, the electrochemical stability of 1.43:1-HT is then investigated by CV using an asymmetric setup with Pt and Na as electrodes. The scan rate and range are 10 mV/s and −1 to 5 V, respectively (Fig. 5). The cathodic and anodic currents can be only observed around 0 V (vs. Na$^+$/Na), indicating the sodium deposition and dissolution, respectively. No significant anodic currents deriving from the decomposition of electrolyte are observed up to 5 V (vs. Na$^+$/Na) and four cycles, which indicates the excellent electrochemical stability of the synthesized composite electrolyte material. The electrochemical stability is much better than other similar hydroborate composite electrolytes, such as Na$_2$(B$_{12}$H$_{12}$)$_{0.5}$(B$_{10}$H$_{10}$)$_{0.5}$, Na$_5$(B$_{11}$H$_{14}$)(B$_{12}$H$_{12}$)$_2$, and Na$_4$(CB$_{11}$H$_{12}$)$_2$(B$_{12}$H$_{12}$) [25,48,49]. Outstanding cyclability of an all-solid-state Na-ion battery using the mixed closo-boride electrolyte is then expectable.

1.43:1-HT is adopted as solid electrolyte to assemble all-solid-state Na-ion battery for its highest ionic conductivity. TiS$_2$ is mixed with 1.43:1-HT in a 60:40 wt% ratio by hand milling to prepare a composite positive electrode and metal Na is used as anode. Then all-solid-state TiS$_2$/1.43:1-HT | 1.43:1-HT | Na battery with bulk type is completed. The as-made battery is repeatedly operated at 0.1°C charge and discharge rates (1°C = 239 mAh/g) and 348 K for more than 100 cycles, as presented in Fig. 6. Two voltage plateaus at ca. 1.2−1.7 V and ca. 2.1−2.3 V vs. Na/Na$^+$ indicate the multistep process of sodium intercalation into TiS$_2$ layer with different stoichiometry of sodium for the formation of Na$_x$TiS$_2$ [26]. The specific discharge capacity of the initial cycle is 276.2 mAh/g, a little more than the theoretical capacity (239 mAh/g) of TiS$_2$. The little larger capacity measured for the initial discharge process is derived from the interfacial reaction between electrolyte and electrode for interface generation, which benefits to smooth charge transfer between positive electrode (TiS$_2$) and electrolyte (1.43:1-HT) [26]. Discharge capacity of the second cycle is as high as 172.9 mAh/g, which is equal to 86.8% Coulombic efficiency, and the battery approximately remains 100% Coulombic efficiency (Fig. S5) after five cycles, implying the charge/discharge reactions take place without significant side reactions and
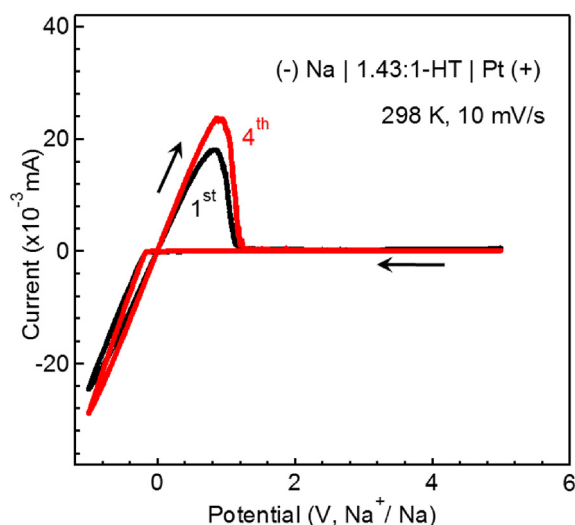

Fig. 5. Cyclic voltammograms of 1.43:1-HT sample sandwiched between Pt and Na as electrodes taken at 298 K with 10 mV/s voltage scan rate over four cycles.
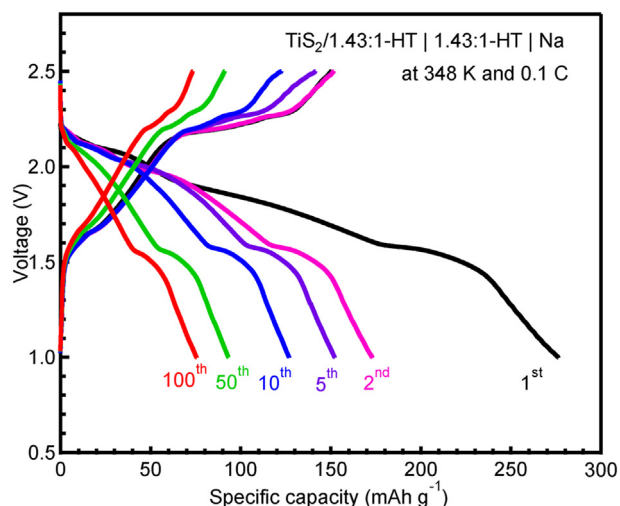
Fig. 6. Charge/discharge profiles over 100 cycles of all-solid-state rechargeable battery TiS$_2$/1.43:1-HT | 1.43:1-HT | Na operated at 348 K and 0.1°C.

indicating that 1.43:1-HT is an excellent solid electrolyte material for practical Na-ion battery application. The battery exhibits a good capacity retention of 93.1/75.4 mAh/g even after 50/100 charge/discharge cycles, which represents a 53.8/43.6% discharge capacity retention ratio evaluated from the second cycle. The capacity degradation is ascribed to the poor electrochemical kinetics and structural stability of TiS$_2$ [50] and the interfacial reaction between TiS$_2$ and 1.43:1-HT as well [26]. Despite all this, the obtained capacity and charge/discharge cycles are much better than partial all-solid-state Na-ion batteries with sulfide, NASICON, or hydroborate electrolytes [26,51−54].

4. Conclusions

In summary, a novel strategy to prepare composite electrolyte for all-solid-state battery use via electrolyte precursor−free approach is proposed and proved to be facile and effective by experiments for the first time. Chemical reactions based on NaNH$_2$ and B$_{10}$H$_{14}$ are adopted for preparing composite electrolyte NaBH$_4$-Na$_2$B$_{12}$H$_{12}$, and a series of composite electrolyte materials with different NaBH$_4$:Na$_2$B$_{12}$H$_{12}$ ratios have been synthesized. Among them, 1.43:1-HT exhibits special core-shell morphology and the highest Na$^+$ conductivity up to 0.1 mS/cm at 373 K. It shows excellent electrochemical stability up to 5 V (vs. Na$^+$/Na), and the all-solid-state Na-ion battery using it as electrolyte reversibly operates for over 100 cycles with 75.4 mAh/g of capacity retention at 348 K and 0.1°C. More advanced composite electrolytes are promising to be developed via reasonable chemical reaction design from different aspects, such as reagent category, starting material ratio, gas pressure, reaction temperature and time, and so on. This study opens a new window for people to design and develop advanced composite electrolytes for next-generation solid battery application.

Authors' contributions

L.H. contributed to investigation, methodology, formal analysis, data curation, visualization, and writing, reviewing, and editing the article. Z.W. contributed to methodology and validation. Y.L. contributed to methodology and visualization. H.L. contributed to investigation. J.L. contributed to validation. T.C. contributed to methodology. Q.Z. contributed to validation. C.S. contributed to

formal analysis. Z.L. contributed to supervision. R.F. contributed to validation. H.-W.L. contributed to supervision, resources, funding acquisition, project administration, and reviewing and editing the article.

Declaration of competing interest

The authors declare that they have no known competing financial interests or personal relationships that could have appeared to influence the work reported in this paper.

Data availability

No data were used for the research described in the article.

Appendix A. Supplementary data

Supplementary data to this article can be found online at https://doi.org/10.1016/j.mtchem.2023.101607.

References

[1] M. Jansen, U. Henseler, Synthesis, structure determination, and ionic conductivity of sodium tetrathiophosphate, J. Solid State Chem. 99 (1) (1992) 110.
[2] R. Murugan, et al., Fast lithium ion conduction in garnet-type Li7La3Zr2O12, Angew. Chem. Int. Ed. 46 (41) (2007) 7778.
[3] V.M. Mohan, et al., Structural, electrical and optical properties of pure and NaLaF4 doped PEO polymer electrolyte films, J. Polym. Res. 14 (4) (2007) 283.
[4] T.J. Udovic, et al., Sodium superionic conduction in Na2B12H12, Chem. Commun. 50 (28) (2014) 3750.
[5] F. Mizuno, et al., Highly ion-conductive crystals precipitated from Li2S-P2S5 glasses, Adv. Mater. 17 (7) (2005) 918.
[6] N. Kamaya, et al., A lithium superionic conductor, Nat. Mater. 10 (9) (2011) 682.
[7] S. Wenzel, et al., Direct observation of the interfacial instability of the fast ionic conductor Li10GeP2S12 at the lithium metal anode, Chem. Mater. 28 (2016) 2400.
[8] Y. Kato, et al., High-power all-solid-state batteries using sulfide superionic conductors, Nat. Energy 1 (2016) 16030.
[9] M. Hou, et al., Challenges and perspectives of NASICON-type solid electrolytes for all-solid-state lithium batteries, Nanotechnology 31 (13) (2020) 132003.
[10] N. Zhao, et al., Solid garnet batteries, Joule 3 (5) (2019) 1190.
[11] M. Matsuo, et al., Complex hydrides with (BH4)- and (NH2)- anions as new lithium fast-ion conductors, J. Am. Chem. Soc. 131 (45) (2009) 16389.
[12] W. Tang, et al., Liquid-like ionic conduction in solid lithium and sodium monocarba-closo-decaborates near or at room temperature, Adv. Energy Mater. 6 (2016) 1502237.
[13] A. Unemoto, et al., Fast lithium-ionic conduction in a new complex hydride-sulphide crystalline phase, Chem. Commun. 52 (3) (2016) 564.
[14] S.A. Hashmi, S. Chandra, Experimental investigations on a sodium-ion-conducting polymer electrolyte based on poly(ethylene oxide) complexed with NaPF6, Mater. Sci. Eng. Adv. Func. Solid State Mater. 34 (1) (1995) 18.
[15] Y.L. Nimah, et al., Solid-state polymer nanocomposite electrolyte of TiO2/PEO/NaClO4 for sodium ion batteries, J. Power Sources 278 (2015) 375.
[16] J.-K. Kim, et al., A hybrid solid electrolyte for flexible solid-state sodium batteries, Energy Environ. Sci. 8 (12) (2015) 3589.
[17] A. Unemoto, et al., Pseudo-binary electrolyte, LiBH4-LiCl, for bulk-type all-solid-state lithium-sulfur battery, Nanotechnology 26 (25) (2015), 254001.
[18] D. Blanchard, et al., Nanoconfined LiBH4 as a fast lithium ion conductor, Adv. Funct. Mater. 25 (2) (2015) 184.
[19] N. Tanibata, et al., X-ray crystal structure analysis of sodium-ion conductivity in 94 Na3PS4·6Na4SiS4 glass-ceramic electrolytes, ChemElectroChem 1 (7) (2014) 1130.
[20] E. Rangasamy, et al., An iodide-based Li7P2S8I superionic conductor, J. Am. Chem. Soc. 137 (4) (2015) 1384.
[21] L. He, et al., Na3NH2B12H12 as high performance solid electrolyte for all-solid-state Na ion batteries, J. Power Sources 396 (2018) 574.

[22] W.S. Tang, et al., Stabilizing superionic-conducting structures via mixed-anion solid solutions of monocarba-closo-borate salts, ACS Energy Lett. 1 (4) (2016) 659.

[23] Y. Sadikin, et al., Superionic conduction of sodium and lithium in anion-mixed hydroborates Na3BH4B12H12 and (Li0.7Na0.3) 3BH4B12H12, Adv. Energy Mater. 5 (21) (2015) 1501016.

[24] L. Duchêne, et al., A highly stable sodium solid-state electrolyte based on a dodeca/deca-borate equimolar mixture, Chem. Commun. 53 (30) (2017) 4195.

[25] L. Duchêne, et al., A stable 3 V all-solid-state sodium–ion battery based on a closo-borate electrolyte, Energy Environ. Sci. 10 (12) (2017) 2609.

[26] K. Yoshida, et al., Fast sodium ionic conduction in Na2B10H10-Na2B12H12 pseudo-binary complex hydride and application to a bulk-type all-solid-state battery, Appl. Phys. Lett. 110 (10) (2017) 103901.

[27] M. Jin, et al., Fast sodium-ion conduction in a novel conjuncto-hydroborate of Na4B20H18, ACS Appl. Energy Mater. 5 (12) (2022) 15578.

[28] Z. Yang, et al., Developing a high-voltage electrolyte based on conjuncto-hydroborates for solid-state sodium batteries, J. Mater. Chem. 10 (13) (2022) 7186.

[29] M. Jin, et al., A novel high-voltage solid electrolyte of Na3B24H23 for 4 V all-solid-state sodium battery, Chem. Eng. J. 455 (2023) 140904.

[30] J. Yang, et al., NASICON-structured Na3.1Zr1.95Mg0.05Si2PO12 solid electrolyte for solid-state sodium batteries, Rare Met. 37 (2018) 480.

[31] Z. Zhang, et al., Na3Zr2Si2PO12: a stable Na+-ion solid electrolyte for solid-state batteries, ACS Appl. Energy Mater. 3 (8) (2020) 7427.

[32] J. Yang, et al., Ultrastable all-solid-state sodium rechargeable batteries, ACS Energy Lett. 5 (9) (2020) 2835.

[33] L. Shen, et al., Flexible composite solid electrolyte with 80 wt% Na3.4Zr1.9Zn0.1Si2.2P0.8O12 for solid-state sodium batteries, Energy Storage Mater. 46 (2022) 175.

[34] H. Wan, et al., Core-shell Fe1-x S@ Na2.9PS3.95Se0.05 nanorods for room temperature all-solid-state sodium batteries with high energy density, ACS Nano 12 (3) (2018) 2809.

[35] H. Wan, et al., Grain-boundary-resistance-less Na3SbS4-xSex solid electrolytes for all-solid-state sodium batteries, Nano Energy 66 (2019) 104109.

[36] H. Wan, et al., Self-formed electronic/ionic conductive Fe3S4@ S@ 0.9 Na3SbS4·0.1 NaI composite for high-performance room-temperature all-solid-state sodium-sulfur battery, Small 16 (34) (2020) 2001574.

[37] H. Wan, et al., Bio-inspired nanoscaled electronic/ionic conduction networks for room-temperature all-solid-state sodium-sulfur battery, Nano Today 33 (2020) 100860.

[38] X. Luo, et al., Core-shell NaBH4@ Na2B12H12 nanoparticles as fast ionic conductors for sodium-ion batteries, ACS Appl. Nano Mater. 5 (1) (2022) 373.

[39] L. He, et al., Facile solvent-free synthesis of anhydrous alkali metal dodecaborate M2B12H12 (M = Li, Na, K), J. Phys. Chem. C 118 (12) (2014) 6084.

[40] L. He, et al., Synthesis of a bimetallic dodecaborate LiNaB12H12 with outstanding superionic conductivity, Chem. Mater. 27 (16) (2015) 5483.

[41] N. Toyama, et al., Lithium ion conductivity of complex hydrides incorporating multiple closo-type complex anions, J. Energy Chem. 38 (2019) 84.

[42] L. He, et al., Facile synthesis of anhydrous Li2B12H12 with high purity by solvent-free method, Inorg. Chim. Acta. 464 (2017) 147.

[43] L. He, et al., A facile solvent-free method for NaBH4 and Na2B12H12 synthesis, Inorg. Chim. Acta. 474 (2018) 16.

[44] M. Matsuo, et al., Sodium and magnesium ionic conduction in complex hydrides, J. Alloys Compd. 580 (2013) S98.

[45] B. Zhong, et al., Hollow BN microspheres constructed by nanoplates: synthesis, growth mechanism and cathodoluminescence property, CrystEngComm 13 (3) (2011) 819.

[46] T. Ohtomo, et al., All-solid-state lithium secondary batteries using the 75Li2S·25P2S5 glass and the 70Li2S·30P2S5 glass-ceramic as solid electrolytes, J. Power Sources 233 (2013) 231.

[47] O. Friedrichs, et al., Role of Li2B12H12 for the formation and decomposition of LiBH4, Chem. Mater. 22 (10) (2010) 3265.

[48] S. Payandeh, et al., Nido-Borate/Closo-Borate mixed-anion electrolytes for all-solid-state batteries, Chem. Mater. 32 (3) (2020) 1101.

[49] R. Asakura, et al., Electrochemical oxidative stability of hydroborate-based solid-state electrolytes, ACS Appl. Energy Mater. 2 (9) (2019) 6924.

[50] C. Huang, et al., Interlayer gap widened TiS2 for highly efficient sodium-ion storage, J. Mater. Sci. Technol. 107 (2022) 64.

[51] A. Hayashi, et al., Superionic glass-ceramic electrolytes for room-temperature rechargeable sodium batteries, Nat. Commun. 3 (2012) 856.

[52] I.-H. Chu, et al., Room-temperature all-solid-state rechargeable sodium-ion batteries with a Cl-doped Na3PS4 superionic conductor, Sci. Rep. 6 (2016) 33733.

[53] F. Murgia, et al., Room-temperature-operating Na solid-state battery with complex hydride as electrolyte, Electrochem. Commun. 106 (2019) 106534.

[54] Y.J. Lim, et al., An epoxy-reinforced ceramic sheet as a durable solid electrolyte for solid state Na-ion batteries, J. Mater. Chem. A 8 (29) (2020) 14528.